Received: 11 November 2019 | Revised: 22 January 2020 | Accepted: 23 January 2020
DOI: 10.1002/poc.4059

RESEARCH ARTICLE

Journal of Physical Organic Chemistry WILEY

Observation of the complex spectra for the supramolecular system involving silver nanoparticles-biaryl Schiff bases containing the nitro group

Chao-Tun Cao | **Shi-Mao Cheng** | **Chenzhong Cao**

Key Laboratory of Theoretical Organic Chemistry and Function Molecule, Ministry of Education, Hunan Provincial University Key Laboratory of QSAR/QSPR, School of Chemistry and Chemical Engineering, Hunan University of Science and Technology, Xiangtan, China

Correspondence
Chenzhong Cao, Key Laboratory of Theoretical Organic Chemistry and Function Molecule, Ministry of Education, Hunan Provincial University Key Laboratory of QSAR/QSPR, School of Chemistry and Chemical Engineering, Hunan University of Science and Technology, Xiangtan 411201, China.
Email: czcao@hnust.edu.cn

Funding information
National Nature Science Foundation of China, Grant/Award Number: 21672058

Abstract

A series of biaryl Schiff bases containing the nitro groups, 4-XArCH=NArNO$_2$-4′ (XBANO$_2$-4′) and 4-NO$_2$ArCH=NArY-4′ (4-NO$_2$BAY), were synthesized. Also, the fish sperm DNA (fsDNA) and silver nanoparticles (AgNPs) solutions were prepared. By mixing these compounds with fsDNA or AgNPs solution and determining the ultraviolet absorption spectra of the mixture solutions, an interesting phenomenon was found: a new absorption peak $\lambda_{\max,\mathrm{lim}}$ appeared in the (XBANO$_2$-4′)-AgNPs solution, which was longer than the wavelength of $\lambda_{\max}$ of XBANO$_2$-4′ solution. The new absorption peak in the (XBANO$_2$-4′)-AgNPs solution was the complex spectrum originating from the electron transfer between XBANO$_2$-4′ and AgNPs. Whereas this phenomenon was not observed in the (4-NO$_2$BAY)-AgNPs solutions, a quantitative correlation analysis was carried out with the measured spectral data, and the results show that the wave number $\nu_{\max,\mathrm{lim}}$ of the $\lambda_{\max,\mathrm{lim}}$ is mainly affected by the excited-state substituent constant $\sigma^{\mathrm{ex}}_{\mathrm{CC}}(X)$ rather than the ground Hammett constant σ of the X group. The redshift magnitude $\Delta\nu_{\max,\mathrm{WSL}}$, namely, $\Delta\nu_{\max,\mathrm{WSL}} = (1/\lambda_{\max}) - (1/\lambda_{\max,\mathrm{lim}})$, of the wavelength $\lambda_{\max,\mathrm{lim}}$ is related to the highest occupied molecular orbital and lowest unoccupied molecular orbital of XBANO$_2$-4′. The discovery of this new phenomenon is helpful to understanding the interaction between AgNPs-organic compound supramolecular systems.

KEYWORDS
complex spectrum, para-nitrobiaryl Schiff base, silver nanoparticles, substituent electronic effect, supramolecular system

1 | INTRODUCTION

The formation of supramolecular systems involving silver nanoparticles (AgNPs) and organic compounds causes significant changes in the optical properties of organic compounds.[1–5] The mechanism of optical properties change attracted many researchers.[6–15] For example, Ashenfelter et al[11] believed that the sulfhydryl (-SH) of glutathione glycopeptide (G-SH) was absorbed by AgNPs to form the interfacial silver-thiolate shell and had strong fluorescence. Wang et al[12] found that the adsorption of the SH functional group of 4-mercaptopyridine (4-MPY) by AgNPs enhanced Raman scattering. Francesko et al, Liu et al, and Miao et al[13–15] designed functionalized silver nanomaterials based on the changes of Raman scattering spectra and redox potential of AgNPs-organic supramolecular system. The supramolecular systems involving AgNPs-organic compounds have been widely used in the detection of biological and organic substances, such as folic acid,[16] antibody[17] and RNA,[18] glutathione, protein and growth factor,[19,20] and mercaptoaniline.[21]

Recently, our group[22] found that in the action of AgNPs, the wavelength of the ultraviolet (UV) absorption spectra of biaryl Schiff bases containing the hydroxyl group shifted with the addition of AgNPs and finally reached a limit value, which could be quantitatively correlated with the electronic effect constants of substituents. However, when we determined the UV spectra of biaryl Schiff bases containing the nitro groups, such as 4-XArCH═NAr NO_2-4′ (XBANO_2-4′), in the action of AgNPs, we observed a new phenomenon; that is, a new absorption peak appeared at the longer wavelength of the UV spectra of Schiff bases. We noted that the biaryl Schiff bases molecules, in our previous works,[22] contained bridging bond C═N, and also, some of them contained hydroxyl group. No one of them contained nitro group. It is not clear whether biaryl Schiff bases containing the nitro groups have any special interaction with AgNPs. Therefore, we want to investigate the UV spectra between AgNPs and Schiff bases containing the nitro groups. In view of this new phenomenon, this paper intends to get meaningful results.

2 | EXPERIMENTS

Fish sperm DNA (fsDNA) was purchased from Boao Bio-Technology Co, Ltd (Shanghai, China). Other chemicals were purchased from J&K Scientific Ltd. All chemicals were of analytic grade and were used as it was received without further purification.

2.1 | Preparation of fsDNA and AgNPs

The preparation of fsDNA solution was as follows. First, 0.1 g of fsDNA was dissolved into 100.0 mL of double-distilled water, and it was heated for 15 minutes in hot water bath at 95°C. Then, the reaction vessel was moved immediately into ice water bath for being cooled rapidly to 4°C. A type of mixed single-strand DNA (ssDNA), namely, the fsDNA solution of 1.0 $g \cdot L^{-1}$, was obtained.

The preparation of AgNPs was carried out according to the methods of our previous work.[22] That is, $AgNO_3$ was reduced by $NaBH_4$, and fsDNA was used as stabilizer. The final concentrations employed were c (ssDNA) = 0.87 $g \cdot L^{-1}$ for fsDNA and c_{Ag} = 0.727 mM for Ag in the AgNPs solution. The size of AgNPs solution was measured by transmission electron microscopy (TEM) (see Figure 1). The average size of AgNPs was about 3.4 nm.

2.2 | Synthesis of MCs

Model compound (MC) 4/4′-NO_2-disubstituted benzylidene aniline *p*-XArCH═NArY-*p* (abbreviated as *p*-XBAY-*p*) was synthesized by the method reported in the literature (see Figure 2).[22–26] The crude products were recrystallized with anhydrous ethanol, and the purified MCs were characterized by ^1H NMR. The NMR spectra were recorded with a Bruker AV 500-MHz spectrometer in $CDCl_3$. The specific data and spectra are available in Data S1.

2.3 | UV spectra of supramolecular system

The MCs XBAYs were vacuum dried for a whole day before measurements. The concentration of MC solution

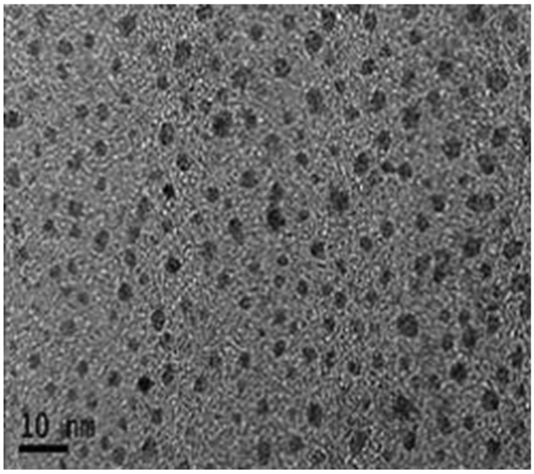

FIGURE 1 Transmission electron microscopy diagram of AgNP solution (taken from[22]). AgNP, silver nanoparticle

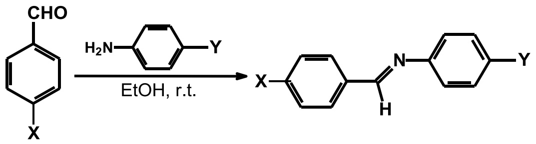

1-12

1-6: X = NMe_2, OMe, Me, F, Cl or CN; Y = NO_2

7-12: X = NO_2; Y = NMe_2, OMe, Me, F, Cl or CN

FIGURE 2 The synthetic route of XBANO_2-4′ and 4-NO_2BAY molecules was 0.727 mM, prepared by dissolving MC in anhydrous ethanol. The UV spectrum of MC solution (total volume was 3 mL; concentration was 1.21×10^{-5} M) was recorded with a ShimadzuUV-1800 spectrophotometer (Japan) at room temperature, and the λ_{max} (nm) was obtained. For each compound-AgNPs (MC-AgNPs) system, firstly, 5 μL of MC solution was added to a set of graduated tubes; the AgNPs solution was subsequently added into the MC solutions, making the MC:Ag molar ratio to be 1:*N* (*N* = 0, 1, 2, ..., 9), and then, the volume was adjusted to 3 mL with anhydrous ethanol. The MC-AgNPs solutions were kept on for 1 hour in avoiding light condition, and then, their UV spectra were recorded. The peaks of $\lambda_{max,mix}$ of the mixing system (MC-AgNPs) were recorded. When the absorption wavelength did not change any more, the solution's peak of $\lambda_{max,mix}$ was taken as the limit wavelength, expressed as $\lambda_{max,lim}$. The measured data were listed in Table 1.

3 | RESULTS AND DISCUSSION

3.1 | Comparison of UV spectra of fsDNA with AgNPs solutions

In order to investigate the variation of UV spectra of fsDNA and AgNPs solutions, we determined the UV spectra of fsDNA and AgNPs solutions with different concentrations (total volume was 3 mL, in which the volumes of fsDNA and AgNPs were going from 5 to 160 μL, respectively). It was shown that the UV spectra of fsDNA and AgNPs solutions did not shift in the above concentration range, yet their absorbance intensities changed for each case.

The UV spectrum of fsDNA had a peak at λ_{max} = 262.0 nm, whereas that of AgNPs had two peaks, one at 263.8 nm and the other at 430.4 nm (λ_{max}). The former belonged to fsDNA, and the latter was caused by AgNPs. Figure 3 is the comparison of UV spectra of fsDNA with AgNPs solutions; there are no absorption peaks in the range of 320 to 400 nm for both fsDNA and AgNPs.

(the absorbance of A and B, from bottom to top, is 5, 10, 20, 40, 80, and 160 μL of fsDNA and AgNPs in 3 mL of anhydrous ethanol, respectively). AgNP, silver nanoparticle; fsDND, fish sperm DNA; UV, ultraviolet

3.2 | Comparison of UV spectra of MC with MC-AgNPs solutions

In order to investigate the shift of λ_{max} of 4-NO_2BAY and XBANO_2-4′ in the presence of AgNPs, we recorded the UV absorption under different ratios of MC:Ag. An interesting phenomenon was observed when the AgNPs solution was mixed with the MC solution.

As regarding the (4-NO_2BAY)-AgNPs solutions, the absorption peak of the original 4-NO_2BAY solution was shifted, but there was no new absorption peak in the direction of longer wavelength of its λ_{max}. For example, the λ_{max} of 4-NO_2BANMe_2-4′ (Figure 4) was 442.3 nm. After it was mixed with the AgNPs solution, no new

TABLE 1 . The λ_{max}, $\lambda_{max,lim}$, and $\Delta\nu_{max,WSL}$ values of MC-AgNPs, and the substituent constants of *X* and *Y* groups

No.	*X*	*Y*	$\sigma_{CC}^{ex}(X)^a$	$\sigma_{CC}^{ex}(Y)^a$	$\sigma_R(X)^b$	$\sigma_R(Y)^b$	$\sigma_F(X)^b$	$\sigma_F(Y)^b$	λ_{max}	$\lambda_{max,lim}$	$\Delta\nu_{max,WSL}{}^c$	ε^d
1	*p*-NMe_2	*p*-NO_2	−1.81	−1.17	−0.98	0.13	0.15	0.65	389.2	405.6	1039	16 500
2	*p*-OMe	*p*-NO_2	−0.50	−1.17	−0.56	0.13	0.29	0.65	346.4	384.6	2867	30 300
3	*p*-Me	*p*-NO_2	−0.17	−1.17	−0.18	0.13	0.01	0.65	331.8	386.2	4245	38 200
4	*p*-F	*p*-NO_2	0.06	−1.17	−0.39	0.13	0.45	0.65	338.4	384.6	3550	37 300
5	*p*-Cl	*p*-NO_2	−0.22	−1.17	−0.19	0.13	0.42	0.65	334.8	381.6	3663	35 100
6	*p*-CN	*p*-NO_2	−0.70	−1.17	0.15	0.13	0.51	0.65	333.1	390.4	4406	21 800
7	*p*-NO_2	*p*-NMe_2	−1.17	−1.81	0.13	−0.98	0.65	0.15	442.3			
8	*p*-NO_2	*p*-OMe	−1.17	−0.50	0.13	−0.56	0.65	0.29	371.8			
9	*p*-NO_2	*p*-Me	−1.17	−0.17	0.13	−0.18	0.65	0.01	353.8			
10	*p*-NO_2	*p*-F	−1.17	0.06	0.13	−0.39	0.65	0.45	340.3			
11	*p*-NO_2	*p*-Cl	−1.17	−0.22	0.13	−0.19	0.65	0.42	345.0			
12	*p*-NO_2	*p*-CN	−1.17	−0.70	0.13	0.15	0.65	0.51	349.2			

Abbreviations: AgNP, silver nanoparticle; MC, model compound.

[a] The values were taken from Hansch et al.[27]

[b] The values were taken from Cao et al, Qu et al, and Zhu et al.[28–30]

[c] It was calculated with the expression: $\Delta\nu_{max,WSL} = 1/\lambda_{max} - 1/\lambda_{max.lim}$.

[d] The molar extinction coefficient of the $\lambda_{max,lim}$, which was calculated on the basis of MC concentration.

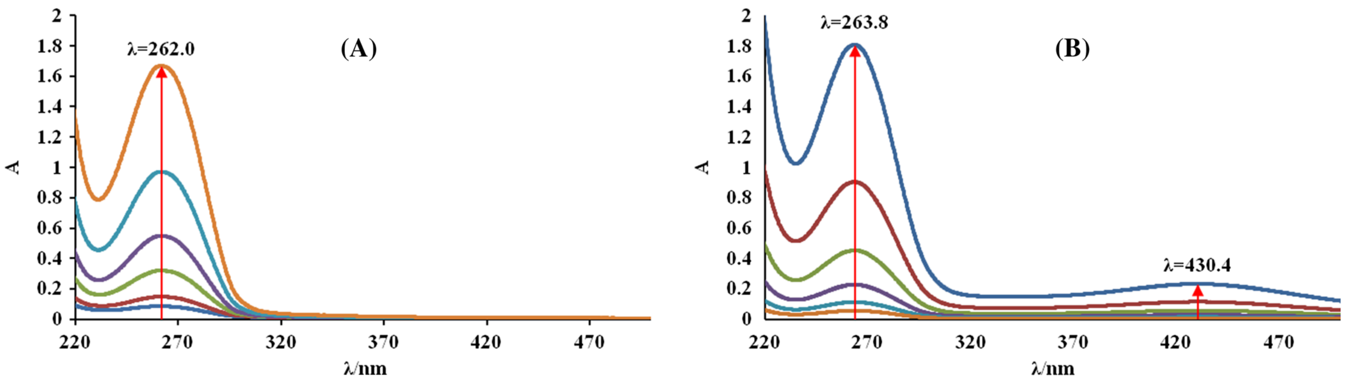

FIGURE 3 The UV spectra of (A) fsDNA and (B) AgNPs in various concentrations

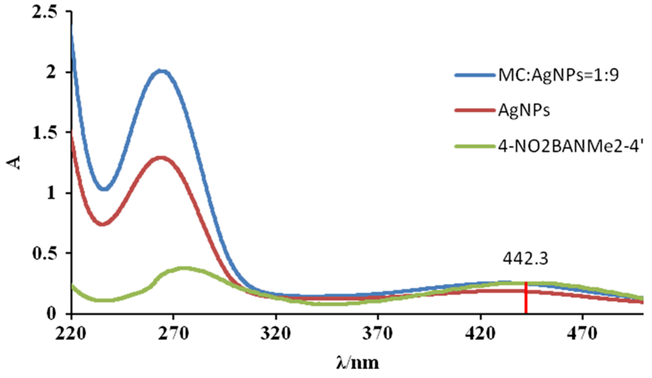

FIGURE 4 The UV spectra of AgNPs, 4-NO_2BANMe$_2$-4′, and (4-NO_2BANMe$_2$-4′)-AgNPs (mole ratio, MC:Ag = 1:9). AgNP, silver nanoparticle; MC, model compound; UV, ultraviolet

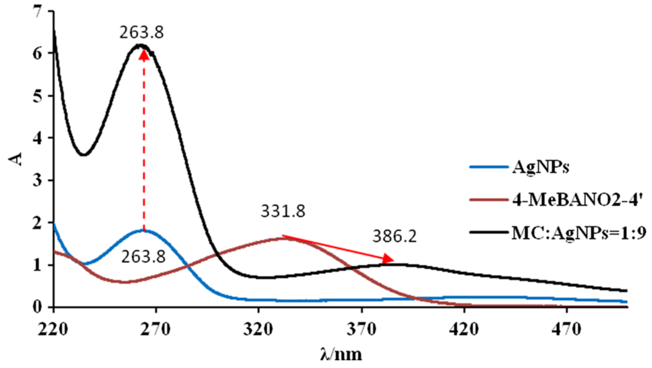

FIGURE 5 The UV spectra of AgNPs, 4-MeBANO$_2$-4′, and (4-MeBANO$_2$-4′)-AgNPs (the arrow "→" indicates the peak shifting of 4-MeBANO$_2$-4′ to (4-MeBANO$_2$-4′)-AgNPs, which was studied in this work). AgNP, silver nanoparticle; UV, ultraviolet

absorption peak appeared in the direction of longer than 442.3 nm.

However, in (XBANO$_2$-4′)-AgNPs solutions, besides the original absorption peaks of XBANO$_2$-4′ shift, a new absorption peak of $\lambda_{\mathrm{max,lim}}$ appeared in the direction of longer wavelength of its λ_{max}, and the original λ_{max} peak disappeared. In the XBANO$_2$-4′ solutions, with the addition of AgNPs solution, the λ_{max} of XBANO$_2$-4′ moved to the longer wave direction (redshift). When the molar ratio of Ag to XBANO$_2$-4′ reached to 9:1, the wavelength did no longer move. This indicated that the MC molecules were basically complexed with AgNPs and underwent intermolecular charge (electron) transfer to produce UV absorption. That is, in case the molar ratio of Ag to MC was above 9:1, the longest wavelength of UV absorption was the absorption peak of MC-AgNPs complex spectrum. Here, we employed the $\lambda_{\mathrm{max,lim}}$ to express the wavelength of the absorption peak and the $\Delta\lambda = \lambda_{\mathrm{max,lim}} - \lambda_{\mathrm{max}}$ to express the displacement (redshift) of the wavelength. Take 4-MeBANO$_2$-4′, for example, Figure 5 is the peak shifting from the UV of 4-MeBANO$_2$-4′ to that of (4-MeBANO$_2$-4′)-AgNPs. Figure 6 is the UV absorption at equal absorbance for (4-MeBANO$_2$-4′)-AgNPs, where 331.8 nm was the λ_{max} of 4-MeBANO$_2$-4′ and 386.2 nm was the $\lambda_{\mathrm{max,lim}}$ of (4-MeBANO$_2$-4′)-AgNPs supramolecular system. Its $\Delta\lambda = 386.2 - 331.8 = 54.4$ nm. The absorption peak at

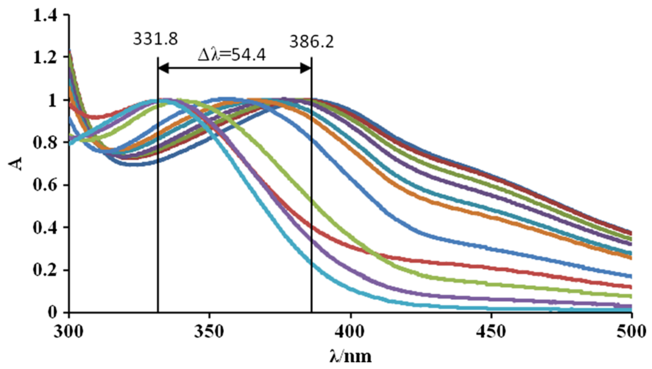

FIGURE 6 The detailed wavelength shift process of (4-MeBANO$_2$-4′)-AgNPs solution at equal absorbance. (From left to right, the mole ratio of MC:Ag was 1:0, 2:1, 1:1, 1:2, 1:3, 1:4, 1:5, 1:6, 1:7, 1:8, and 1:9, respectively). AgNP, silver nanoparticle; MC, model compound

386.2 nm was a new absorption peak, which was not observed in the UV spectrum of 4-MeBANO$_2$-4′ or AgNPs solution, respectively. Moreover, when the molar ratio of Ag to 4-MeBANO$_2$-4′ reached to 9:1, the absorption intensity (absorbance) of the peak of 386.2 nm did not increase. It could be reasonably explained that the concentration of MC-AgNPs supramolecular complex in MC-AgNPs supramolecular solution depended on the original concentration of MC in the system, rather than excess AgNPs. When all 4-MeBANO$_2$-4′ molecules were complexed with the AgNPs, the absorbance of (4-MeBANO$_2$-4′)-AgNPs supramolecular system remained unchanged.

From Table 1, it could be concluded that the minimum redshift of compounds **1-6** was 16 nm (4-Me$_2$NBANO$_2$-4′) and the maximum was 57 nm (4-CNBANO$_2$-4′), and the redshift was very obvious. It is noteworthy that the $\lambda_{\max,\lim}$ of (XBANO$_2$-4′)-AgNPs complex spectra has no linear relationship with the $\lambda_{\max}$ of XBANO$_2$-4′ UV absorption.

The detailed peak shift process for all MC-AgNPs solutions (nos **1-12** of Table 1) can be seen in Data S1.

We want to know whether the $\lambda_{\max}$ shifting of XBANO$_2$-4′ originates from the interaction of fsDNA or AgNPs. Thus, we mixed the XBANO$_2$-4′ and fsDNA to form the (XBANO$_2$-4′)-fsDNA solution then recorded the UV spectra of (XBANO$_2$-4′)-fsDNA solutions under different volume ratios. It was observed that there was no $\lambda_{\max}$ shifting of XBANO$_2$-4′ in the (XBANO$_2$-4′)-fsDNA solution. For example, Figure 7 is the UV spectra of fsDNA, 4-MeBANO$_2$-4′, and (4-MeBANO$_2$-4’)-fsDNA solutions, where the $\lambda_{\max}$ of 4-Me-BANO$_2$-4′ did not change as the addition of the fsDNA solution. The above experimental results indicated that the $\lambda_{\max}$ shifting of X-BANO$_2$-4′ was originated indeed from the action of AgNPs rather than the action of fsDNA.

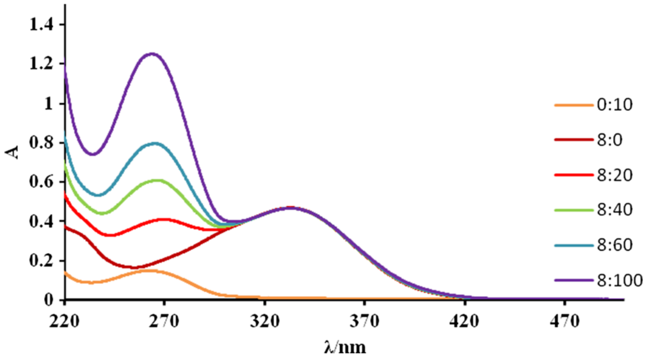

FIGURE 7 The UV spectra of fsDNA (0:10),4-MeBANO$_2$-4′ (8:0), and (4-MeBANO$_2$-4′)-fsDNA solutions under different volume ratios (from MC:fsDNA = 8:20 to 8:100 μL). fsDNA, fish sperm DNA; MC, model compound; UV, ultraviolet

The above experimental facts showed that the $\lambda_{\max}$ of XBANO$_2$-4′ appeared redshift in the (XBANO$_2$-4′)-AgNPs supramolecular system, whereas the $\lambda_{\max}$ of 4-NO$_2$BAY did not appear redshift in the (4-NO$_2$BAY)-AgNPs system. It means that the $\lambda_{\max}$ redshift in MC-AgNPs depend on the position of nitro group attached to the biaryl Schiff base molecule.

Do other compounds with strong electron-withdrawing groups (such as 4-CNBAY-4′ and 4-XBACN-4′) have similar behavior? Recently, we studied on the UV spectra of supramolecular system involving 38 samples of (*p*-XBAY-*p*) excluding OH, NH$_2$, and SH groups, in which both 4-CNBAY-4′ and 4-XBACN-4′ all did not appear $\lambda_{\max}$ redshift in the action of AgNPs.[31] It implies that the $\lambda_{\max}$ redshift is the specific behavior of XBANO$_2$-4′ in the action of AgNPs.

3.3 | Quantitative correlation of supramolecular complex spectra of MC-AgNPs

According to our previous report,[32,33] the $\nu_{\max}$ (cm^{-1}, $\nu_{\max} = 1/\lambda_{\max}$) of Schiff bases could be quantitatively correlated with Hammett constant σ and the excited-state substituent constant σ^{ex}_{CC}. For compounds **1-6** in Table 1, the $\lambda_{\max,\lim}$ was converted to $\nu_{\max,\lim}$. Because the substituent parameters of substituent NO$_2$ in molecules 4-XBANO$_2$-4′ is fixed, we correlated quantitatively these $\nu_{\max,\lim}$ values with the substituent parameters $\sigma^{ex}_{CC}(X)$, $\sigma_R(X)$, and $\sigma_F(X)$ of the substituents *X*, respectively. The results indicated that the correlations between $\nu_{\max,\lim}$ and $\sigma_R(X)$ or $\sigma_F(X)$ all were bad, and the correlation between $\nu_{\max,\lim}$ and $\sigma^{ex}_{CC}(X)$ was good, as shown in Equation (1). It could be seen that the complex spectra of (XBANO$_2$-4′)-AgNPs supramolecular system were mainly affected by the excited-state substituent constant $\sigma^{ex}_{CC}(X)$ of the *X* group but not by the Hammett constant σ of the *X* group. Positive $\sigma^{ex}_{CC}(X)$ value makes $\nu_{\max,\lim}$ increase and $\lambda_{\max,\lim}$ shorten; negative $\sigma^{ex}_{CC}(X)$ value makes $\nu_{\max,\lim}$ decrease and $\lambda_{\max,\lim}$ lengthen.

$$\begin{aligned} \nu_{\max,\lim} &= 26\,168.66 + 790.88\sigma^{ex}_{CC}(X) \\ R &= 0.9445, S = 205.68, F = 33.08, n = 6. \end{aligned} \tag{1}$$

In order to investigate the factor of affecting the wavelength redshift in going from the $\lambda_{\max}$ of MC to the $\lambda_{\max,\lim}$ of (XBANO$_2$-4′)-AgNPs, we used $\Delta\nu_{\max,WSL}$ to express the difference of wavenumber between them; that is, $\Delta\nu_{\max,WSL} = (1/\lambda_{\max}) - (1/\lambda_{\max,\lim})$. It is an interesting topic that what is the factor of dominating the

$\Delta\nu_{max,WSL}$. We think it may be related to the molecular frontier orbital of both MC and AgNPs. Here, we employed the $HOMO_{MC}$ and $HOMO_{AgNPs}$ to express the highest occupied molecular orbital (HOMO) of MC and AgNPs respectively and the $LUMO_{MC}$ and $LUMO_{AgNPs}$ for the lowest unoccupied molecular orbital (LUMO) of them, respectively. Dewar et al[34] and Pysh et al[35] ever pointed out that the charge transfer spectra of π-complexes were resulted from the charge transfer, in which the electron transfer is going from the HOMO of donor to the LUMO of acceptor. According to this view, we think that the $\lambda_{max,lim}$ should be originated in the electron transfer from the $HOMO_{AgNPs}$ to the $LUMO_{MC}$ or from the $HOMO_{MC}$ to the $LUMO_{AgNPs}$. Thus, the $\Delta\nu_{max,WSL}$ may be expressed as Equation (2).

$$\Delta\nu_{max,WSL} = k\left[\left(LUMO_{MC} - HOMO_{AgNPs}\right) + \left(LUMO_{AgNPs} - HOMO_{MC}\right)\right]. \tag{2}$$

Here, k is coefficient. Equation (2) also can be rewritten as Equation (3).

$$\Delta\nu_{max,WSL} = k\left[\left(LUMO_{MC} - HOMO_{MC}\right) + \left(LUMO_{AgNPs} - HOMO_{AgNPs}\right)\right]. \tag{3}$$

Since the $LUMO_{AgNPs}$ and $HOMO_{AgNPs}$ of AgNPs are fixed, the item ($LUMO_{AgNPs} - HOMO_{AgNPs}$) is a constant. The item ($LUMO_{MC} - HOMO_{MC}$) is indeed the energy of λ_{max} of MC, which can be expressed as the ν_{max}. Thus, Equation (3) may be expressed as Equation (4).

$$\Delta\nu_{max,WSL} = a + b\left(LUMO_{MC} - HOMO_{MC}\right) = a + b\nu_{max}, \tag{4}$$

where a is constant and b is coefficient. Equation (4) indicates that the $\Delta\nu_{max,WSL}$ can be correlated with the $LUMO_{MC}$ and $HOMO_{MC}$ of MC. Therefore, we used the ν_{max} values of compounds **1-6** in Table 1 to correlate their $\Delta\nu_{max,WSL}$ of ($XBANO_2$-4′)-AgNPs, and obtained Equation (5).

$$\begin{gathered}\Delta\nu_{max,WSL} = -17\,329 + 0.710593\nu_{max}\\ R = 0.9755, S = 303.34, F = 78.7, n = 6.\end{gathered} \tag{5}$$

Equation (5) has good correlation, which shows that $\Delta\nu_{max,WSL}$ is affected by the ν_{max} of $XBANO_2$-4′. The larger ν_{max} of $XBANO_2$-4′ will result in a greater $\Delta\nu_{max,WSL}$ of ($XBANO_2$-4′)-AgNPs and a greater redshift from the λ_{max} of MC to the $\lambda_{max,lim}$ of MC-AgNPs.

From Equation (2), we can see that what the λ_{max} of $XBANO_2$-4′ appears redshift in ($XBANO_2$-4′)-AgNPs should have proper energy of $LUMO_{MC}$ and $HOMO_{MC}$ (lower energy of $LUMO_{MC}$ and higher energy of $HOMO_{MC}$). In the $XBANO_2$-4′ molecule, because of the strong electron-withdrawing effect of both the nitro group and the bridge bond CH═N, the π electrons flow strongly from the aldehyde aryl to the aminoaryl when the *X* group is electron-donating group. it is favorable for the positive charges distributing on the aldehyde aryl (decreasing the energy of $LUMO_{MC}$, or increasing electron acceptability), which makes the aldehyde aryl ring more receptive to the electron transfer from $HOMO_{AgNPs}$. Also, it is favorable for the negative charges distributing on the nitro group (increasing electron donor capability of oxygen anion O^-), which makes the nitro group of MC easier transfer the electron to the $LUMO_{AgNPs}$. Figure 8 is the diagram of the π electron transfer in the MC molecules. The above analysis can be confirmed by the reduction potential E_{Red} of compound XBAY. It was known that the reduction potentials of organic compounds depend on the energy of the LUMO. On the basis of the quantitative equation of reduction potential of XBAY, reported by Luo et al[36] (formula 6, herein) and Cao et al,[37] we calculated the reduction potentials E_{Red} of compounds **1-6** in Table 1 and got the E_{Red} values, −2.101, −1.988, −1.978, −1.898, −1.789, and −1.538 V, respectively. It indicates that the LUMO energy of 4-NMe_2BANO_2-4′ is lower than that of 4-$CNBANO_2$-4′, and the former is easier to accept electron transfer from $HOMO_{AgNPs}$ than the latter does. Figure 9 was obtained

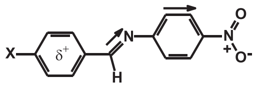

FIGURE 8 The π electron transfer of molecules $XBANO_2$-4′ (the arrow "→" indicates the direction of π electron transfer)

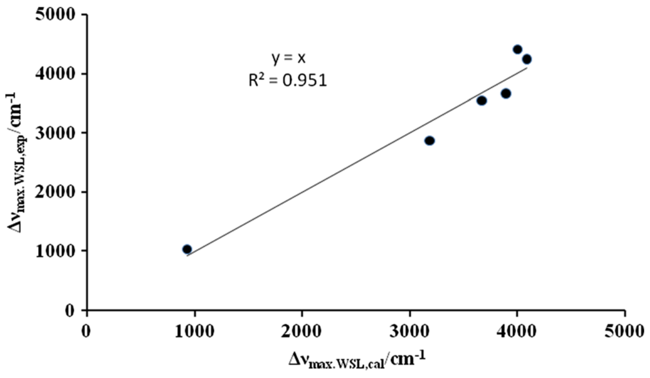

FIGURE 9 Plot of the calculated $\Delta\nu_{max.WSL,cal}$ with Equation (5) versus the experimental $\Delta\nu_{max,WSL,exp}$ values

by plotting the experimental values versus the calculated values of $\Delta\nu_{\mathrm{max.WSL}}$ of Equation (5). We can see, from Figure 9, that the calculated values are in good agreement with the experimental values.

The experimental results of this work show that the absorption peak of 4-NO_2BAY is not longer than the λ_{max} wavelength of 4-NO_2BAY in the action of AgNPs, which indicates that there is no electron transfer between 4-NO_2BAY and AgNPs. The reason is still unclear and needs further study.

4 | CONCLUSION

By studying the UV spectra of a series of biaryl Schiff bases containing the strong electron- withdrawing group (NO_2) to strong electron-donating group (NMe_2) and AgNPs, we can get the following conclusions:

1. An intermolecular complex spectrum may be generated between the nitro-containing biaryl Schiff base and the AgNPs, which is related to the position of the nitro group attached to.
2. The compound 4-NO_2BAY has no intermolecular complex spectrum in the action of AgNPs.
3. The compound XBANO_2-4′ produces intermolecular complex spectrum in the action of AgNPs rather than fsDNA. Its longest wavelength $\lambda_{\mathrm{max,lim}}$ has a quantitative relationship with the substituent constant of the *X* substituent. Compared with the λ_{max} of XBANO_2-4′, the redshift Δλ of intermolecular complex spectrum $\lambda_{\mathrm{max,lim}}$ is related to the highest occupied molecular orbital $\mathrm{HOMO_{MC}}$ and lowest unoccupied molecular orbital $\mathrm{LUMO_{MC}}$ of MC.
4. The UV spectrum of the (XBANO_2-4′)-AgNPs supramolecular system is different from these of supramolecular systems involving AgNP-substituted *N*-(phenyl-ethylene)-anilines[38] and AgNPs-biaryl Schiff bases containing hydroxyl.[22] The discovery of this new phenomenon is conducive to understanding the interaction between AgNPs-organic compound supramolecular systems.

ACKNOWLEDGMENT

Authors is very grateful to the National Nature Science Foundation of China (21672058).

ORCID

Chenzhong Cao https://orcid.org/0000-0001-5224-7716

REFERENCES

[1] E. B. Santos, F. A. Sigoli, I. O. Mazali, *Vib. Spectrosc.* **2013**, *68*, 246. https://doi.org/10.1016/j.vibspec.2013.08.003

[2] L. Marsich, A. Bonifacio, S. Mandal, S. Krol, C. Beleites, V. Sergo, *Langmuir* **2012**, *28*, 13166. https://doi.org/10.1021/la302383r

[3] W. Song, Y. X. Wang, B. Zhao, *J. Phys. Chem. C* **2007**, *111*(34), 12786. https://doi.org/10.1021/jp073728b

[4] R. Chadha, N. Maiti, S. Kapoor, *J. Mol. Struct.* **2014**, *1076*, 35. https://doi.org/10.1016/j.molstruc.2014.07.042

[5] T. W. H. Oates, Y. Shiratori, S. Noda, *J. Phys. Chem. C* **2009**, *113*, 9588. https://doi.org/10.1021/jp900436a

[6] Y. Y. Chen, C. Wang, H. Y. Liu, J. S. Qiu, X. H. Bao, *Chem. Commun.* **2005**, *37*(42), 5298. https://doi.org/10.1039/b509595f

[7] R. W. Y. Sun, R. Chen, P. Y. Chung, C. M. Ho, C. L. S. Lin, C. M. Che, *Chem. Commun.* **2005**, *40*(40), 5059. https://doi.org/10.1039/b510984a

[8] A. M. Whelan, M. E. Brennan, W. J. Blau, J. M. J. Kellya, *Nanosci. Nano* **2004**, *4*(1-2), 66. https://doi.org/10.1166/jnn.2004.054

[9] J. P. Wilcoxon, B. L. Abramsb, *Chem. Soc. Rev.* **2006**, *35*(11), 1162. https://doi.org/10.1039/b517312b

[10] J. Zheng, Y. Ding, B. Z. Tian, Z. L. Wang, X. W. Zhuang, *J. Am. Chem. Soc.* **2008**, *130*(32), 10472. https://doi.org/10.1021/ja803302p

[11] B. A. Ashenfelter, A. Desireddy, S. H. Yau, T. Goodson, T. P. Bigioni, *J. Phys. Chem. C* **2015**, *119*, 20728. https://doi.org/10.1021/acs.jpcc.5b05735

[12] X. K. Wang, L. Chen, X. L. Fu, L. X. Chen, Y. J. Ding, *ACS Appl. Mater. Inter.* **2013**, *5*(21), 11059. https://doi.org/10.1021/am404142e

[13] A. Francesko, L. Blandon, M. Vazquez, P. Petkova, J. Morato, A. Pfeifer, T. Heinze, E. Mendoza, T. Tzanov, *ACS Appl. Mater. Inter.* **2015**, *7*, 9792. https://doi.org/10.1021/acsami.5b01670

[14] Z. Y. Liu, Y. X. Hu, *ACS Appl. Mater. Inter.* **2016**, *8*, 21666. https://doi.org/10.1021/acsami.6b06727

[15] P. Miao, K. Han, H. X. Sun, J. Yin, J. Zhao, B. D. Wang, Y. G. Tang, *ACS Appl. Mater. Inter.* **2014**, *6*, 8667. https://doi.org/10.1021/am501473m

[16] C. F. Hu, Y. L. Liu, J. L. Qin, J. T. Nie, B. F. Lei, Y. Xiao, M. T. Zheng, J. H. Rong, *Acs Appl. Mater. Inter.* **2013**, *5*(11), 4760.

[17] H. Li, W. B. Qiang, M. Vuki, D. K. Xu, H. Y. Chen, *Anal. Chem.* **2011**, *83*(23), 8945.

[18] R. Salahandish, A. Ghaffarinejad, E. Omidinia, H. Zargartalebi, K. Majidzadeh-A, S. M. Naghib, A. Sanati-Nezhad, *Biosens. Bioelectron.* **2018**, *120*, 129.

[19] Y. Bu, G. X. Zhu, S. L. Li, R. G. Qi, G. Bhave, D. C. Zhang, R. X. Han, D. L. Sun, X. F. Liu, Z. B. Hu, X. W. Liu, *Acs Appl. Nano Mater.* **2017**, *1*(1), 410.

[20] H. Li, M. Wang, C. Z. Wang, W. Li, W. B. Qiang, D. K. Xu, *Anal. Chem.* **2013**, *85*(9), 4492.

[21] L. W. Nien, M. H. Chien, B. K. Chao, A. J. Chen, J. H. Li, *J. Phys. Chem. C* **2016**, *120*(6), 3448.

[22] C.-T. Cao, S. M. Cheng, J. Y. Zhang, C. Z. Cao, *J. Phys. Org. Chem.* **2019**, *32*(3), e3910. https://doi.org/10.1002/poc.3910

[23] C. T. Cao, Y. K. Bi, C. Z. Cao, *Spectrochim. Acta A* **2016**, *163*, 96.

[24] C. Z. Cao, B. T. Lu, G. F. Chen, *J. Phys. Org. Chem.* **2011**, *24*, 335.

[25] L.-y. Wang, C.-t. Cao, C.-z. Cao, *Chin. J. Chem. Phys.* **2016**, *29*, 260.

[26] L. Wang, C.-T. Cao, C. Z. Cao, *J. Phys. Org. Chem.* **2016**, *29*, 299.

[27] C. Hansch, A. Leo, R. W. A. Taft, *Chem. Rev.* **1991**, *91*(2), 165. https://doi.org/10.1021/cr00002a004

[28] C.-T. Cao, H. Yuan, Q. Zhu, C. Z. Cao, *J. Phys. Org. Chem.* **2019**, *32*(8), e3962. https://doi.org/10.1002/poc.3962

[29] J. Y. Qu, C.-T. Cao, C. Z. Cao, *J. Phys. Org. Chem.* **2018**, *31*(5), e3799. https://doi.org/10.1002/poc.3799

[30] Q. Zhu, C.-T. Cao, C.-Z. Cao, *Acta Phys.-Chim. Sin.* **2017**, *33* (4), 729. https://doi.org/10.3866/PKU.WHXB201611291

[31] C.-T. Cao, S.-M. Cheng, C.-Z. Cao, *Chem. Res. Appl.* **2019**, *31* (9), 1635.

[32] C.-T. Cao, W. Zhou, C. Z. Cao, *J. Phys. Org. Chem.* **2017**, *30*, e3672. https://doi.org/10.1002/poc.3672

[33] Z. J. Fang, C. Z. Cao, *J. Mol. Struct.* **2013**, *1036*, 447.

[34] M. J. S. Dewar, A. R. Lepley, *J. Am. Chem. Soc.* **1961**, *83*, 4560.

[35] E. S. Pysh, N. C. Yang, *J. Am. Chem. Soc.* **1963**, *85*, 2124.

[36] Q.-Q. Luo, C.-T. Cao, C.-Z. Cao, *Acta Phys.-Chim. Sin.* **2016**, *32* (7), 1691. https://doi.org/10.3866/PKU.WHXB201604061

[37] C.-T. Cao, W. Zhou, C. Cao, *J. Phys. Org. Chem.* **2019**, e4028. https://doi.org/10.1002/poc.4028

[38] C.-T. Cao, J. Liu, C. Cao, *J. Phys. Org. Chem.* **2019**, *32*(10), e3993. https://doi.org/10.1002/poc.3993

SUPPORTING INFORMATION

Additional supporting information may be found online in the Supporting Information section at the end of this article.

How to cite this article: Cao C-T, Cheng S-M, Cao C. Observation of the complex spectra for the supramolecular system involving silver nanoparticles-biaryl Schiff bases containing the nitro group. *J Phys Org Chem*. 2020;e4059. https://doi.org/10.1002/poc.4059